Journal of
Materials Chemistry C

PAPER

View Article Online
View Journal | View Issue

Cite this: J. Mater. Chem. C, 2015, 3, 3038

Cyanostilbene bent-core molecules: a route to functional materials†

M. Martínez-Abadía,[a] B. Robles-Hernández,[b] B. Villacampa,[c] M. R. de la Fuente,[b] R. Giménez*[a] and M. B. Ros*[a]

Received 20th January 2015,
Accepted 3rd February 2015

DOI: 10.1039/c5tc00201j

www.rsc.org/MaterialsC

The synthesis and characterization of novel compounds, that incorporate the high current interest functional cyanostilbene unit, are reported. Four examples, derived from 3,4′-biphenylene, have a 2D molecular-shape that promotes a variety of bent-core liquid crystalline phases (columnar, polar smectic C, and dark-conglomerate phases). The mesomorphism has been characterized by optical microscopy, differential scanning calorimetry, X-ray diffraction, and by detailed electrooptic and dielectric studies. The liquid crystalline properties can be modulated depending on the position of the cyano group on the C=C bond (α- or β-isomers) and the number of cyanostilbene units in the molecule (one or two). The polar smectic C mesophases have an antiferroelectric ground state. Furthermore, the multiresponsive nature of the cyanostilbene structure has led to very attractive and diverse photoactivity, including luminescence and second harmonic generation. The results obtained broaden the possibilities for the use of bent-core liquid crystals to design novel multiresponsive soft materials.

Introduction

Since 1996[1] new types of liquid crystalline materials have been added to the classical rod-like and disk-like varieties, namely bent-core liquid crystals (BCLC), which have been widely studied in the liquid crystals field and the soft matter area.[2–13] The compact packing afforded by bent-shaped molecules leads to the formation of unconventional mesophases, many of which are still being investigated. These novel mesophases are usually either lamellar or columnar in nature but, interestingly, many variants have been reported due to the presence of undulated or modulated arrangements, or tilted and non-tilted molecular dispositions, among other possibilities.

The polar smectic C mesophase (SmCP or B_2) is probably the most common and best known phase of this type and it helps to show the richness of this kind of BCLC.[14] The SmCP phase is characterized by a tilted lamellar structure. Within each layer the bent molecular shape restricts the rotation of the molecules around their long axes, thus giving rise to polar layers in which the polarization of neighboring layers is usually antiparallel and the corresponding mesophases are antiferroelectric in the ground state. Furthermore, depending on the tilt sense of the molecules in adjacent layers, this soft phase could be racemic (SmC_sP_A) or homochiral (SmC_aP_A), with the latter leading to differentiated chiral domains, as in the case of the dark conglomerate phase (DC). This mesophase has provided materials with very attractive functional properties[15–17] such as ferro- and antiferroelectric switching[14] and piezoelectric[18,19] or nonlinear optical responses.[20–26] These properties arise due to the molecular non-centrosymmetric order, which attractively is achieved using achiral molecules. Interestingly, in some cases a ferroelectric ground state has been reported for these materials.[27] Due to the strong tendency of the electric polarization to splay, the flat layers of the lamellar phases might become unstable leading to the formation of 2D density modulated phases. There are structures in which the layers are undulated or even completely frustrated, which leads to the formation of columnar phases (for example the Col_r or B_1).[28–30]

In the last decade a great deal of attention has been focused on other phases based on bent-core molecules, such as the nematic bent-core mesophase, which has provided a route to the elusive biaxial nematic materials,[11,31] or the dark conglomerate-forming mesophases. The dark phases can be smectic phases (DC, sponge-like phase)[32] or soft crystalline helical nanofilament phases (HNF or B_4 phases).[33,34] The B_4 phase is neither a traditional crystalline solid nor a conventional liquid crystal; it is characterized by its

[a] Instituto de Ciencia de Materiales de Aragón (ICMA), Departamento de Química Orgánica-Facultad de Ciencias, Universidad de Zaragoza-CSIC, 50009 Zaragoza, Spain. E-mail: rgimenez@unizar.es, bros@unizar.es
[b] Departamento de Física Aplicada II, Facultad de Ciencia y Tecnología, Universidad del País Vasco UPV/EHU, 48080 Bilbao, Spain
[c] Instituto de Ciencia de Materiales de Aragón (ICMA), Departamento de Física de la Materia Condensada-Facultad de Ciencias, Universidad de Zaragoza-CSIC, 50009 Zaragoza, Spain

† Electronic supplementary information (ESI) available: Detailed synthetic procedures and characterization data, NMR spectra, DSC thermograms, XRD diffractograms, UV-Vis absorption and fluorescence spectra, and dielectric and electrooptic data for α,α-B. See DOI: 10.1039/c5tc00201j

spontaneous twist to form a helical structure. In the sponge-type DC phases, layers without in-plane order are strongly deformed in a non-regular way, so that uniformly oriented regions become smaller than the wavelength of light. In both cases the mesophases appear to be optically isotropic. Thus, in addition to the aforementioned properties, BCLCs, through their variety of molecular compact packings, offer high expectations for both supramolecular chemistry and materials science in the search for innovative functional materials for technological applications.

In the field of functional organic materials π-conjugated luminophores are being widely studied because of their structural diversity and unique photophysical properties. Moreover, these studies have been intensified to achieve multiresponse systems.[35–37] Within this family it is worth highlighting the cyanostilbene chromophore[38,39] [–Ar–CH=C(CN)–Ar–], which is easily accessible by chemical synthesis and is able to show photoactivity, tunable fluorescence, and the phenomenon of aggregation-induced enhanced emission (AIEE),[38,40,41] thus allowing applications in biological imaging,[42,43] optical storage,[44–50] and optoelectronic devices (OLEDs, OFETs, solar cells),[51–55] promising a new generation of multifunctional materials. The excellent characteristics of the cyanostilbene chromophore can be combined with those of liquid crystals.[44,49,56–65] In particular, this combination of properties remains unexplored with BCLCs. Moreover, in the literature there are very few examples in which the luminescence properties of compounds with bent-core type mesophases have been reported.[66–70] This situation makes these systems novel not only for the design of new photoactive functional materials but also with the aim of using them as fluorescent probes for mesophase characterization.[69]

Herein we describe several bent-shaped molecules that incorporate the cyanostilbene structure with the aim of promoting bent-core liquid crystalline phases and to explore their multifunctional capabilities (Fig. 1). A set of isomers has been prepared and these differ in the position of the cyano group (–CN) in the C=C with respect to the carboxylate link (–COO–), *i.e.*, α-position [–Ar–CH=C(CN)–Ar–COO–] or β-position [–Ar–C(CN)=CH–Ar–COO–], and the number of cyanostilbene units (1 or 2). There are two mono-cyanostilbene bent-shaped compounds, named α-B and β-B, and two di-substituted ones, α,α-B and β,β-B (B denotes the bent-core structure). In order to induce bent-core mesophases, the 3,4′-biphenylene system was selected as the central core. The cyanostilbene structure is used here for the first time in bent-core liquid crystals. The aim was to study the influence of this unit on the formation of bent-core mesophases and also to assess the photoactivity of this kind of molecule by studying the UV-Vis absorption, fluorescence and nonlinear optical properties.

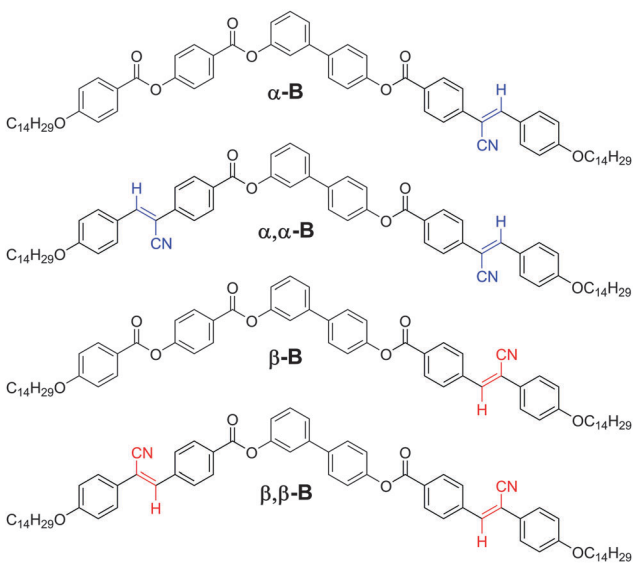

Fig. 1 Chemical structures of compounds with one [α-B, β-B] and two [α,α-B and β,β-B] cyanostilbene [–Ar–CH=C(CN)–Ar–] units.

Results and discussion

Synthesis

The novel bent-core compounds were synthesized by the synthetic procedures outlined in Schemes 1 and 2 for precursors and final compounds, respectively. In all cases, synthetic methods for similar intermediates or adapted for the target compounds were followed. Experimental details and structural characterization of the compounds are described in the ESI.†

In order to incorporate the luminescent unit in the bent-shaped molecules, the preparation of different cyanostilbene-containing carboxylic acids (compounds α-A and β-A, where A denotes the acid structure) was carried out. Furthermore, for comparative purposes ester analogs α-E and β-E (E denotes the ester structure) were also synthesized. These intermediates (α-A, β-A, α-E, and β-E) were obtained by Williamson reactions on *p*-hydroxybenzaldehyde (for α-compounds) or on *p*-hydroxyphenylacetonitrile (for β-compounds), followed by a Knoevenagel condensation[40,58] with the appropriate methyl benzoate. In the case of the acids (α-A, β-A), potassium hydroxide was used as a base to hydrolyze the methyl ester simultaneously, while potassium *tert*-butoxide was needed for the ester-intermediates

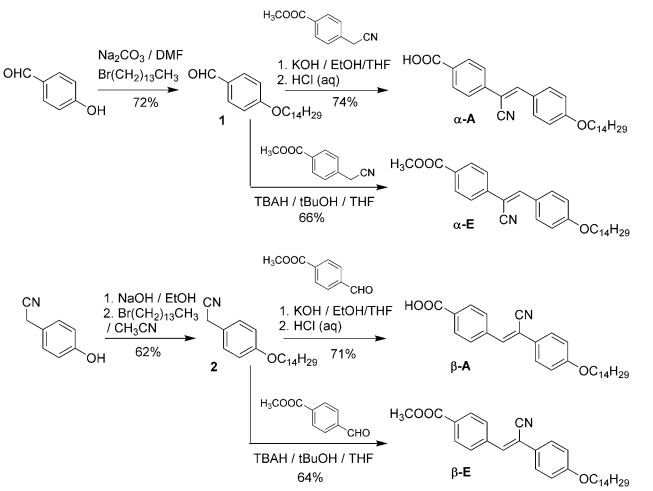

Scheme 1 Synthetic routes for the preparation of the rod-like cyanostilbenes.

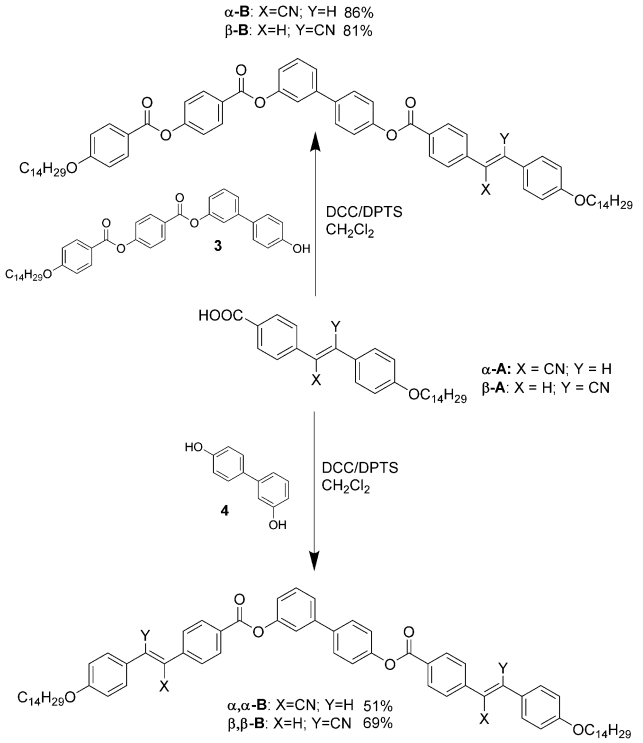

Scheme 2 Synthetic routes for the preparation of the bent-core cyanostilbenes.

(α-E, β-E). The target bent-shaped compounds α-B and β-B were synthesized by esterification of the cyanostilbene acids (α-A or β-A) with compound **3** (Scheme 2).[71,72] Compounds α,α-B and β,β-B were synthesized by esterification with 3,4′-dihydroxybiphenyl (**4**). In both cases, *N*,*N*′-dicyclohexylcarbodiimide (DCC) and *p*-(*N*,*N*-dimethylamino)pyridinium *p*-toluensulfonate (DPTS) were used for efficient condensation steps.

In accordance with previous reports,[73,74] the photosensitivity of the cyano-compounds was evident in solution. As a consequence, the synthesis and purification of these cyanostilbenes should be carried out with protection from ambient light. In fact, if reactions are carried out under ambient light, a mixture of $Z + E$ isomers is obtained and a reverse to the *Z*-isomer can only be achieved by recrystallization or by heating the compounds under reflux in *p*-xylene with I_2 as a catalyst.[74]

Liquid crystalline and electro-optical properties of the materials

All of the new cyanostilbene compounds were studied by optical microscopy between crossed polarizers (POM) using an optical 400 nm longpass filter on the light source, differential scanning calorimetry (DSC), and X-ray diffraction (XRD) in order to characterize the liquid crystalline behavior. Furthermore, detailed dielectric and electrooptic studies were performed in order to obtain additional information about the liquid crystalline phases formed by these molecules. The results obtained using the different techniques allowed us to assign the liquid crystalline phases and these are listed in Table 1.

Optical textures. POM observations at different temperatures showed that the carboxylic acids α-A and β-A display enantiotropic smectic C (SmC) mesophases along with complex crystalline polymorphism, as revealed by DSC. For the esters, only α-E is mesomorphic and this exhibits enantiotropic smectic A (SmA) and nematic (N) mesophases. In general, the textures observed by POM were typical for these mesophases (Fig. 2a–d) and these phases were confirmed by XRD.

Interestingly, all bent-core cyanostilbenes showed complex crystalline polymorphism and the original as-obtained crystal phase was not recovered after the first cooling cycle, as evidenced by DSC. The final phase obtained upon cooling at 10 °C min^{-1} was always crystalline but this showed complex behavior in the subsequent heating cycle, which can include cold recrystallizations and other crystal-to-crystal transitions. A simplified version of the thermal transitions is collected in Table 1, and detailed information is shown in the ESI.† Cooling cycles were reproducible and only the first one is shown. Quite interestingly, for most bent-core compounds a rapid cooling process allowed the mesophase arrangement to be frozen at room temperature (see below).

The results of POM studies show that the four bent-core molecules promote the formation of bent-core liquid crystalline phases with broad ranges. In the case of compound β-B textures typical of a polar smectic C mesophase (SmCP) were observed (Fig. 2e). Upon cooling compound α-B at a very slow rate from the isotropic liquid (Instec cells) a banana-leaf texture formed and this was reminiscent of that shown by some columnar phases (Fig. 3). This texture was broken upon cooling and finally, below 120 °C, resembled the typical SmCP texture, although a clear change at a particular temperature could not be observed by POM or DSC. This compound will be discussed further in terms of the electric field effects on the textures.

Several remarkable differences were observed in the case of the bent compounds bearing two cyanostilbene units. For example, a texture typical of a SmCP mesophase was obtained (Fig. 4a) upon heating compound β,β-B whereas a dark conglomerate (DC) texture with chiral domains was detected upon cooling the material from the isotropic liquid (Fig. 4b–d). Furthermore, slower cooling rates led to the formation of larger chiral domains. Finally, compound α,α-B, in contrast to the previous compounds, only displayed a fan-shaped texture after melting at 134 °C consistent with a columnar mesophase (Fig. 2f). In the second heating cycle at 10 °C min^{-1}, this compound showed unconventional behavior in that the melting point was lowered by 27 °C, giving rise to a intermediate phase (X phase in Table 1) that changed at 132 °C to a Col_r phase with very small enthalpy but in a very reproducible way. This intermediate phase X seems to be an unstable SmCP phase, which recrystallizes to Cr upon heating (see below and ESI†), and its existence depends on the thermal history of the sample as slower heating only leads to a crystal phase. However, in the cooling process only the columnar mesophase is observed down to the crystallization point.

Structural characterization. XRD data for all mesomorphic compounds are shown in Table 1. Diffractograms have been included in the ESI.†

Table 1 Liquid crystal characterization data for the cyanostilbene compounds

Compound	Phase transitions[a,b] T/°C (ΔH/kJ mol^{-1})	Mesophase (T/°C of XRD data)	d/Å	Miller index	Parameters/Å
α-A	Cr 142 (11.9) SmC 229 (10.8) I I 227 (10.8) SmC 139 (11.6) Cr	SmC (160)	41.1	001	c = 41.1
β-A	Cr 131 (26.7) SmC 218 (11.2) I I 215 (10.8) SmC 125 (24.8) Cr	SmC (145)	41.1	001	c = 41.1
α-E	Cr 96 SmA 99 N 101 (61.0)[c] I I 100 N 98 (2.6)[c] SmA 87 (49.4) Cr	SmA (104)	35.2	001	c = 35.2
β-E	Cr 103 (65.7) I I 97 (59.5)[c] Cr	—	—	—	—
α-B	Cr 89 (53.3)[c] $SmCP_A$ 148[d] Col_r 164 (18.1) I I 160 (18.1) Col_r 115[d] $SmCP_A$ 33 (8.7) Cr Cr 86 (2.6) $SmCP_A$ 148[d] Col_r 163 (16.7) I	$SmCP_A$ (110) Col_r (152)	44.8 22.4 15.0 44.8 26.0 22.4	001 002 003 101 002 202	c = 44.5 a = 88.7 c = 51.9
β-B	Cr 93 (61.3) $SmCP_A$ 167 (23.7) I I 164 (23.2) $SmCP_A$ 45 (15.9) Cr Cr 90 (39.1) $SmCP_A$ 166 (23.4) I	$SmCP_A$ (131)	44.8 22.4 15.0	001 002 003	c = 44.5
α,α-B	Cr 134 (58.3) Col_r 191 (20.3) I I 188 (20.0) Col_r 89 (87.2) Cr Cr 107 (88.8)[c] X[e] 132 (0.7) Col_r 190 (19.9) I	Col_r (147)	51.9 39.4 26.0	101 002 202	a = 68.9 c = 78.9
β,β-B	Cr 134 (46.7)[c] $SmCP_A$ 177 (23.2) I I 174 (22.1) DC 106 (55.5) Cr Cr 133 (49.8)[c] $SmCP_A$ 177 (22.2) I	DC-$SmCP_A$ (160)	44.8 22.4	001 002	c = 44.8

[a] Data determined by DSC, temperatures at the maximum of the peaks from the first heating and cooling cycle at a scanning rate of 10 °C min^{-1}, additionally the second heating cycle is shown for bent-core compounds. Cr: crystal phase, SmC: smectic C mesophase, SmA: smectic A mesophase, N: nematic mesophase, $SmCP_A$: antiferroelectric polar smectic C mesophase, DC: dark conglomerate mesophase, Col_r: rectangular columnar mesophase, I: isotropic liquid. [b] The crystal phase denoted as Cr is, in most cases, not unique and crystalline polymorphism with complex transitions appears (see thermograms in the ESI). [c] Combined enthalpy of several crystalline transitions. [d] Data obtained from dielectric spectroscopy. [e] Depends on the thermal history, at 10 °C min^{-1} is an unstable SmCP mesophase which recrystallizes to Cr upon heating.

The rod-like acid precursors α-A and β-A exhibit diffraction patterns that are consistent with SmC mesophases with a layer thickness of around 41 Å. This is longer than the calculated molecular length for an all-*trans* conformation, which is around 32 Å. It is known that benzoic acids usually form dimers through hydrogen bonding and the mesophase could be formed by such dimers arranged in tilted layers.

In the case of the ester precursor, α-E, the nematic phase could not be studied by XRD due to the short range over which it appeared. The mesophase that formed upon cooling the nematic phase was assigned as SmA. The measured layer thickness (35.2 Å) is again longer than the calculated molecular length for an all-*trans* conformation (32 Å) and this, in conjunction with the absence of dimerization by hydrogen bonding, means that the mesophase has a partial bilayer structure in which molecules are arranged in an antiparallel and partially interdigitated manner.

The diffraction patterns for bent-core compounds β-B and α-B in their SmCP mesophases are very similar. In the wide angle region a diffuse scattering suggests the absence of any in-plane order. In the small angle regions there are three sharp reflections, which can be indexed as the (001), (002), and (003) reflections of a lamellar phase. These patterns are indicative of a well-defined layer structure in the mesophase, where the molecules are tilted within the layers given that their molecular length (about 71 Å in an all-*trans* conformation) is longer than the measured interlayer distance (44 Å).

The diffraction pattern for compound α-B at temperatures above 148 °C is not typical of a lamellar structure, but it contains reflections that reveal a 2D translation lattice of a columnar mesophase. This situation could arise through undulation (or some sort of frustration) of the smectic layers, which would result in a columnar-type phase with very strong lamellar character. This kind of behavior has been reported to be compatible with a simple Col_r–SmCP transition mechanism in which the blocks in the (101) pseudolayers of the columnar structure stretch to conform to the smectic layers in the SmCP phase.[29]

The diffraction pattern of the mesophase of β,β-B shows two reflections in the small angle region and these are assigned to (001) and (002) of a lamellar packing with a layer parameter similar to that in β-B. A DC mesophase can be proposed despite the lower number of reflections. Detailed freeze-fracture transmission electron microscopy (FFTEM) studies carried out on this material confirmed this assignment.[75]

Finally, the diffraction pattern for compound α,α-B above 134 °C shows several sharp reflections in the small angle region that do not correspond to a lamellar structure, but can be attributed to a columnar mesophase with a rectangular unit cell (Col_r). This phase remains upon cooling until crystallization.

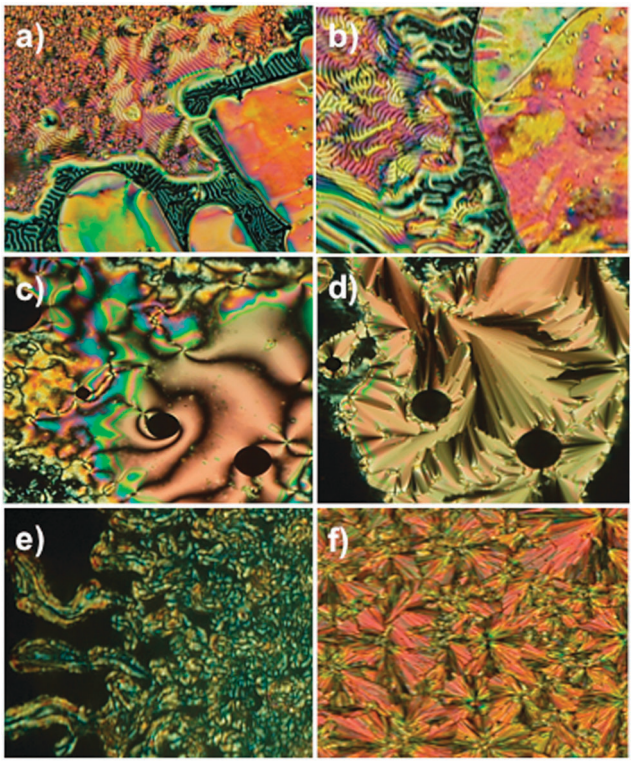

Fig. 2 Microphotographs of the textures between crossed polarizers. (a) SmC phase of α-A at 218 °C. (b) SmC phase of β-A at 211 °C; (c) and (d) N and SmA phase for α-E at 97 °C and 94 °C respectively; (e) SmCP phase of β-B at 148 °C; (f) Col_r phase texture at 166 °C for compound α,α-B.

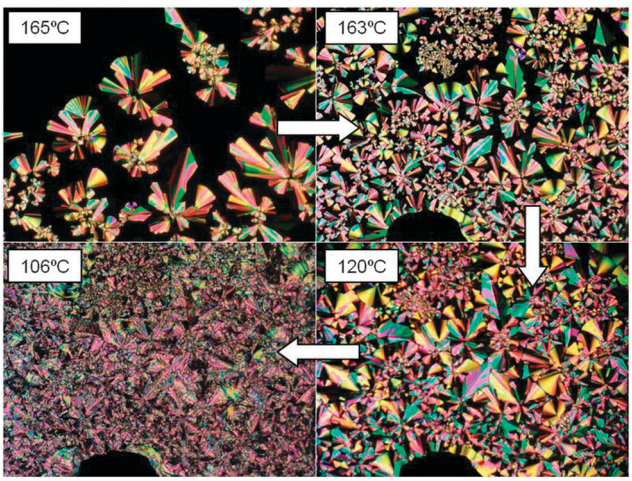

Fig. 3 Microphotographs of the textures displayed by α-B between crossed polarizers in the cooling process.

It is interesting to note that XRD experiments indicate that the SmCP mesophases of β-B and α-B, along with the DC mesophase of β,β-B, can be vitrified at room temperature by a fast cooling process.

Dielectric and polarization studies. Compounds α-B, β-B, α,α-B, and β,β-B were studied under triangular electric fields (50 Hz) in order to analyze the polar switching and by dielectric spectroscopy; representative results are presented in this section.

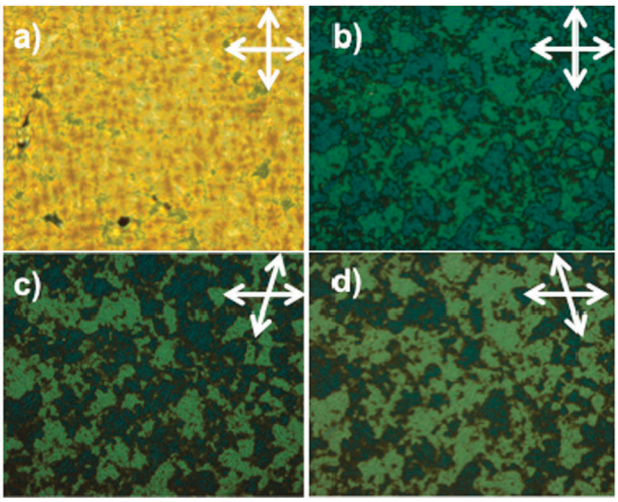

Fig. 4 Microphotograph of the texture obtained for compound β,β-B: (a) crossed polarizers at 144 °C upon heating, (b) crossed polarizers at 175 °C upon cooling; (c) and (d) slightly uncrossed polarizers (right and left, respectively) at 175 °C upon cooling showing domains of different chirality of the DC phase.

Firstly, compounds β-B and β,β-B will be considered. Both materials exhibit typical antiferroelectric behavior with saturated polarization values around 600 nC cm^{-2} and 700 nC cm^{-2}, respectively. The current profile for compound β-B is shown in Fig. 5a, where two peaks per half cycle can be observed. Three-dimensional plots of the dielectric losses *vs.* frequency and temperature recorded upon cooling under isothermal conditions and at a dc voltage of 40 V (gold electrodes, 50 μm) are shown in Fig. 5b (β-B) and c (β,β-B). After applying a fitting procedure (see ESI†), the strengths and frequencies of the most relevant modes were obtained. A plot of the strengths *vs.* temperature is shown in Fig. 5d and an Arrhenius plot of these frequencies *vs.* temperature is shown in Fig. 5e. In the isotropic phase there is a mode at around 10 MHz and this is attributed to the rotation around the molecular long axis. For both compounds in the corresponding lamellar phase (SmCP or DC-SmCP) the spectrum is dominated by a mode whose frequency is around 1 MHz just below the isotropic phase. It seems a continuation of the isotropic mode but it is much stronger than one would expect. Similar modes have been reported in lamellar phases and are attributed to collective fluctuations of polar order. The strength depends significantly on the field treatment and such behavior has also been reported previously.[18,76] Another mode at higher frequency is also present in both compounds. This high frequency mode could be due to the motions of the terminal chains.

Compound α-B is discussed below. A three-dimensional plot of the losses *vs.* temperature and frequency is shown in Fig. 6a. A change at around 115 °C can clearly be observed although DSC experiments did not show evidence of any phase transition. After a fitting procedure, the frequencies and strengths of the most relevant modes are presented in Fig. 6b (Arrhenius plot) and c (*vs.* temperature). As for the previous two compounds, there is a mode in the isotropic phase and a high frequency mode over the whole studied temperature range. The assignment of these

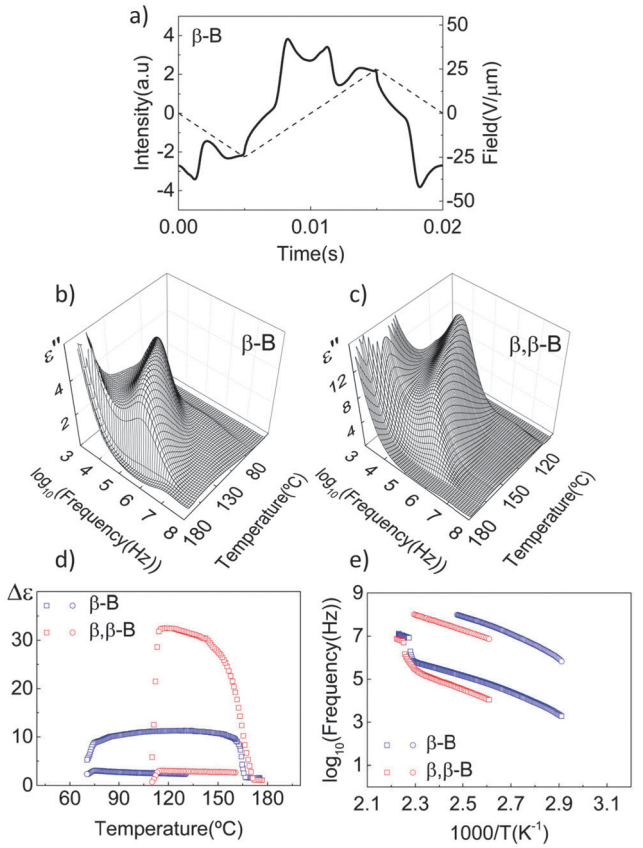

Fig. 5 (a) Polarization switching current of compound β-B at 153 °C, triangular field 50 Hz. (b) Three-dimensional plot of the dielectric losses *vs.* temperature and frequency for β-B. (c) Three-dimensional plot of the dielectric losses *vs.* temperature and frequency for β,β-B. (d) Amplitudes of the relaxation modes *vs.* temperature: in blue color β-B(○,□) and in red color β,β-B(○,□). (e) Arrhenius plot of the frequency of the relaxation modes: in blue color β-B(○,□) and in red color β,β-B(○,□).

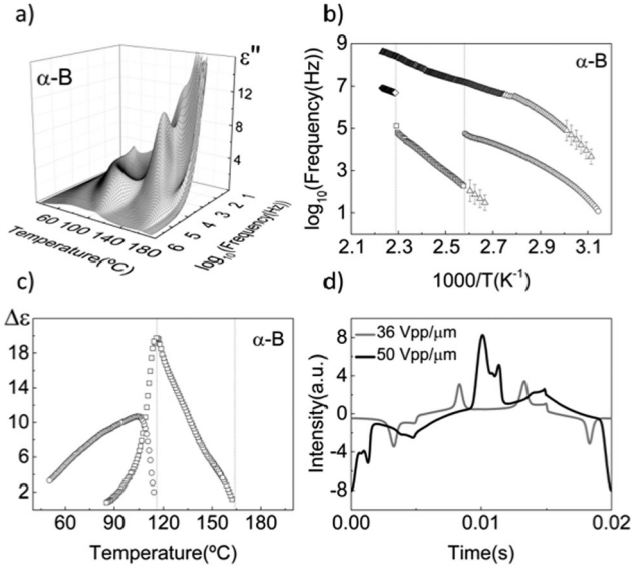

Fig. 6 Studies on compound α-B (a) three-dimensional plot of the dielectric losses *vs.* temperature and frequency, gold cell 50 μm. (b) Arrhenius plot of the frequency of the relaxation modes. (c) Amplitudes of the low frequency modes *vs.* temperature. (d) Switching response at 163 °C, triangular field 50 Hz.

modes is the same as described above. In the high temperature mesophase there is another mode at a much lower frequency and with a higher strength, which reaches a value of around 20 on approaching the SmCP phase, after which it decreases sharply. At the same time a mode at an intermediate frequency, two decades higher, appears and its strength rapidly increases to a value of around 12. Both modes are thermally activated and they decrease in frequency very rapidly, as can be seen in the three-dimensional plot (Fig. 6a) and in Fig. 6b. We believe that both modes could arise for the same reason: namely, collective fluctuations of polar order. As mentioned above, based on optical textures and XRD data, this high temperature mesophase has a columnar character with blocks of layers. It has been reported[30,77] that this structure is related to thermal distortion of the antiparallel arrangement of the dipole moments in the consecutive layers and that, when defects in the layers appear due to the interaction with the block boundaries, the amplitude of the dielectric response should decrease and its relaxation frequency increase when compared to the situation in the SmCP lamellar phase. However, in our case the opposite occurred: the frequency decreased as the strength increased. Very similar behavior has been observed for other compounds that show the phase sequence I–Col$_r$–SmCP.[78,79] We believe that the high temperature mesophase – although it exhibits some 2D periodicity – is strongly lamellar, as described for compound Ic in a publication by Gimeno *et al.*[79] Moreover, although the transition from the high temperature mesophase to SmCP is first order in nature (with a noticeable thermal hysteresis), the enthalpy content should be almost zero (in our case it was not detected by DSC measurements).

The switching and polarization behavior of this compound in the SmCP phase is similar to that of the previous two compounds, β-B and β,β-B. However, in the high temperature mesophase under strong electric fields there were some similarities with the two compounds described by Ortega *et al.*[78] and Gimeno *et al.*[79] There is a clear critical field above which the depolarization current appears, initially as well separated small bumps that merge upon increasing the field strength, see Fig. 6d (note that the horizontal axis is time). The textural changes that occur upon increasing the field are shown in Fig. 7: from a texture very similar to the columnar phases to a texture reminiscent of the SmCP phase. The latter corresponds to the texture that remained when the field was switched off. The curve in Fig. 6d corresponding to high field is similar to that obtained at lower temperatures in the SmCP phase. It seems that the switching occurs in a structure similar to this lamellar phase.

In the case of compound α,α-B, in the Col$_r$ phase switching or depolarization current were not observed at fields as strong as 70 V μm^{-1}. For the dielectric permittivity studies, a three-dimensional plot of the losses *vs.* temperature and frequency, and an Arrhenius plot of the frequency of the observed modes are included in the ESI.† Although the strengths are much lower, the frequency of the low frequency mode in the Col$_r$ phase coincides with that observed in the high temperature

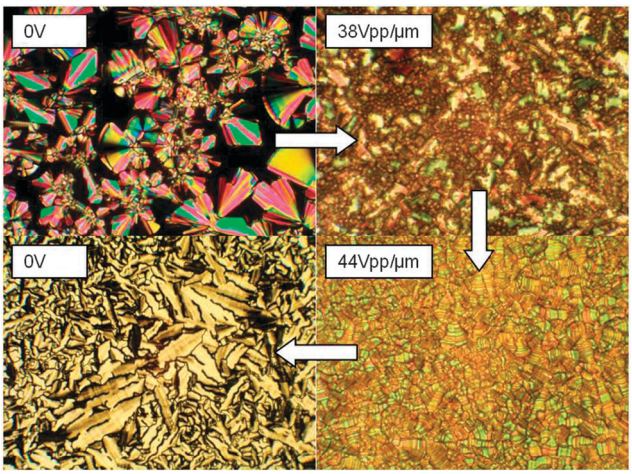

Fig. 7 Evolution of textures under triangular wave fields, 50 Hz, for compound α-B.

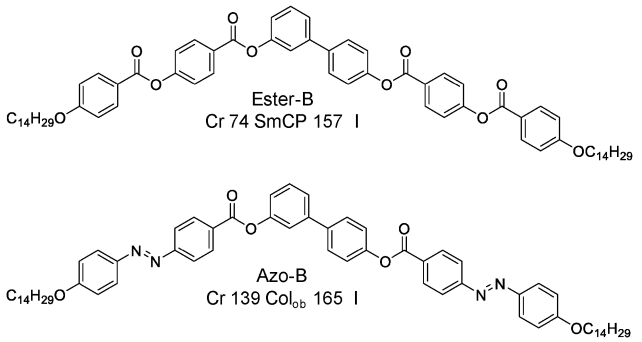

Fig. 8 Chemical structure and liquid crystalline properties of compounds ester-B and azo-B.

mesophase of α-B, a finding that supports our proposed columnar character for the mesophase of compound α-B. In the unstable phase obtained in the second heating between 107 °C and 132 °C (X phase in Table 1) the dielectric permittivity changed in a different way depending on the thermal history, with different behavior observed when the measurements were carried out with a thermal ramp or stepwise (see ESI†). Upon applying a thermal ramp the process at 107 °C could be assigned to a change to a SmCP phase that is crystallizing. Under electric fields a change in the texture that is similar to SmCP switching is observed, although the polarization current is very small and depends strongly on the frequency. Upon applying a stepwise ramp the change at 107 °C is a crystal-to-crystal transition similar to that observed by XRD.

Structure–activity relationship. The cyanostilbene unit has the ability to induce liquid crystal mesophase formation and, in general, it also promotes a rich crystal polymorphism, either for rod-like or bent-shaped compounds.

As expected for benzoic acids, these compounds exhibit broad mesophase ranges and very high mesophase stabilization in comparison to their ester analogs due to the formation of hydrogen-bonded dimers.

All of the 3,4′-biphenylene derivatives exhibit liquid crystalline phases that are characteristic of bent-core compounds. Textures, XRD patterns, electrooptic responses, and enthalpy values for the mesophase-to-isotropic liquid transition, in the range 20–30 kJ mol^{-1}, are also consistent with this type of system. Once again the marked ability of this core to induce and stabilize this type of mesophase has been demonstrated.

Several interesting conclusions can be drawn regarding the influence of the presence of the cyanostilbene unit [–Ar–CH=C(CN)–Ar–]. Firstly, when only one unit is included, the differences between the α- or β-cyanostilbene structure are not very significant in terms of the type of mesophase or the transition temperatures. However, the effect of α- *versus* β-cyanostilbene structures is more marked upon increasing the number of cyanostilbene units to two. Whereas compound β,β-B has the shortest mesophase range and a lamellar mesophase, α,α-B strongly stabilizes both the liquid crystal order, as this compound has the highest clearing temperature of the series, and the columnar arrangements rather than a lamellar organization.

Secondly, comparison of the mesomorphic properties of these four bent-core compounds with those of other 3,4′-biphenyl homologs[22,23,71] shows that the presence of the cyanostilbene unit in the lateral structure of the bent-core compounds can be used to modulate the liquid crystalline properties of bent-shaped molecules by changing both the position of the cyano group and the number of cyanostilbene units. Thus, the presence of just one cyanostilbene core afforded very similar properties to the ones exhibited by the all-ester 3,4′-biphenyl homolog[23,71] (ester-B, Fig. 8). However, while α,α-B has a significantly stabilized mesophase organization in comparison with ester-B, the isomer β,β-B is more similar to the di-azo-analog[22] (azo-B, Fig. 7) as far as the transition temperatures and range of mesophase are concerned. Thus, the presence of two cyano groups in an inner position of the lateral structure (as in α,α-B) leads to stronger molecular interactions, which in turn interestingly favour the stabilization of mesomorphic order into ribbons in a periodic 2D lattice (Col$_r$ type mesophases) rather than a layered organization (SmCP type mesophases).

Optical properties

As mentioned above, the interest in this research was two-fold. One aim was to gain further insights into the structure–activity relationships for cyanostilbene-containing bent-core liquid crystals. Furthermore, we also aimed to assess the photoactivity due to the multiresponse that this structure could offer: fluorescence, nonlinear optical activity and photochemical processes. With the latter aim in mind, we describe below a study of the optical properties in solution in order to evaluate the potential of these novel structures.

UV-Vis absorption and fluorescence. One of the attractive features of the cyanostilbene structure is its fluorescence. The absorption and emission data for the novel rod-like and bent-core cyanostilbenes are shown in Table 2.

It can be seen from the similar absorption profiles that the cyanostilbene unit absorbs in the 350 nm region (Fig. 9),

Table 2 UV-Vis absorption and fluorescence properties[a]

Compound	λ_{abs}/nm	$\varepsilon/10^4$ L mol^{-1} cm^{-1}	λ_{em}/nm	Φ_{PL}[b]
α-A	264, 354	0.6, 3.3	436	<0.001
β-A	263, 351	1.0, 2.5	445	0.07
α-E	263, 354	0.7, 3.3	434	<0.001
β-E	264, 349	0.8, 2.6	440	0.08
α-B	267, 356	4.0, 3.3	442	<0.001
β-B	267, 354	5.5, 3.1	450	0.08
α,α-B	267, 358	3.0, 7.8	442	<0.001
β,β-B	264, 353	3.4, 6.0	450	0.08

[a] Dichloromethane solution. [b] Quantum yields calculated using 9,10-diphenylanthracene in cyclohexane as reference (Φ_{PL} = 0.9).[82]

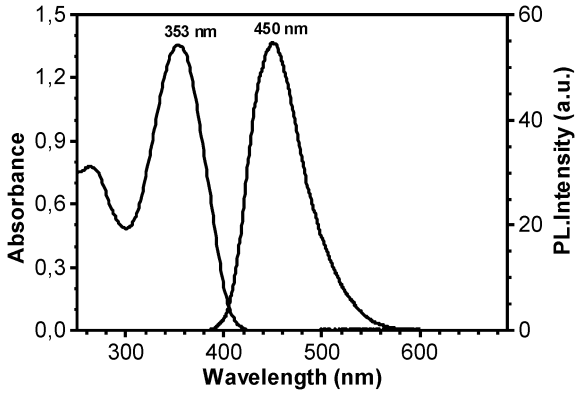

Fig. 9 Absorption and fluorescence spectra of β,β-B in dichloromethane.

with only slight differences observed depending on the position of the cyano group on the C=C bond. A bathochromic shift occurs upon changing from the β- to the α-isomers and an increase in the molar absorptivity is observed, indicating stronger charge-transfer character for the cyanostilbene unit in the α-position.

The fluorescence spectra show clear differences in intensity, with the α-isomers being much less fluorescent. The quantum yields obtained for the β-isomers are one order of magnitude higher (7–8%) than those of the α-isomers (below 1%). These low values have been attributed to non-radiative deactivation pathways of the cyanostilbene chromophore involving intramolecular vibrations and rotations, which are favored in liquid solutions.[38,80,81] Therefore, the deactivation pathways should be more favoured in the case of α-isomers. Slight differences in the emission maxima were also observed, with a bathochromic shift evident on going from the α- to the β-isomers, although it should be noted that the low intensity of the former could distort the spectra and the measurement of the emission maxima.

Nonlinear optical properties. In previous studies[22–24] we analyzed the NLO activity, namely second harmonic generation (SHG), of different series of bent-core liquid crystals. It was concluded that the bent molecular shape is appropriate for the design of NLO materials. Furthermore, the degree of polar stereocontrol achievable with this kind of material is also very good and is better than those achieved with poled polymers or rod-like ferroelectric liquid crystals.

Table 3 Nonlinear optical properties of some of the rod-like and bent-core cyanostilbenes[a]

Compound	$\mu\beta \times 10^{-48}$/esu	$\mu\beta_0 \times 10^{-48}$/esu
α-E	100 (±20)	50 (±10)
β-E	85 (±5)	43 (±4)
α-B	180 (±30)	80 (±20)
β-B	200 (±30)	100 (±20)
α,α-B	280 (±20)	135 (±10)
β,β-B	260 (±40)	130 (±20)
Ester-B	40 (±15)[b]	36 (±15)

[a] EFISH measurements carried out in chloroform at 1064 nm. $\mu\beta_0$ values extrapolated at zero frequency using a simple two level dispersion model. [b] Measurement performed at 1907 nm in dichloromethane.

The presence of the cyanostilbene group in the lateral structures allows a delocalized electronic charge distribution between the donor and acceptor groups along the whole separation distance and provides the opportunity to assess the nonlinear (NLO) efficiencies of these new bent-core molecules. The ability of these compounds to generate nonlinear optical responses was explored at both the molecular and macroscopic level. With this aim in mind, the first hyperpolarizabilities of these bent-shaped molecules and the cyanostilbene esters α-E and β-E (1D-analogs of the lateral structures of the bent-core compounds) were measured in solution by the Electric Field Induced Second Harmonic (EFISH) generation technique. The results are gathered in Table 3.

It can be seen that cyanostilbene structures connecting weak donor and acceptor groups, such as those present in our molecules, afford SHG activity due to moderate hyperpolarizabilities ($\mu\beta_0$: 80–135 × 10^{-48} esu). Interestingly, the incorporation of these D–π–A systems (NLO-phores) in a 2D-structure leads to an increase in the SHG molecular activity in comparison with the 1D-esters. This increase is more marked when two cyanostilbene cores are present. Nevertheless, the position of the cyano group on the double bond does not have a marked effect on this response. However, both cyanostilbene structures have significantly improved NLO responses in these molecules in comparison to ester-B.

All attempts to perform SHG monodomain measurements on the $SmCP_F$ phase proved unsuccessful, a situation that prevented measurement of the characteristic NLO parameters *d* and *D*. Nevertheless, the EFISH values at the molecular level measured for the cyanostilbene bent-core compounds reported here are higher to those measured for ester-B. Thus, bearing in mind the fact that the NLO-parameters in the mesophase measured for ester-B are *d*: 1.2 pm V^{-1} and *D*: 2 pm V^{-1}, at 1.064 nm,[23] it seems reasonable that the incorporation of cyanostilbene units in bent-shaped molecules should allow attractive NLO-materials to be obtained.

Summary and conclusions

The potential of incorporating the high current interest cyanostilbene unit into bent-core molecules has been demonstrated and these units are suitable to impart bent-core liquid crystals with desirable properties.

The presence of a 3,4′-biphenylene central core means that these compounds have a 2D-shape that promotes bent-core mesophases regardless of the position of the CN group on the C═C bond (α or β-isomers) or the number of cyanostilbene units in the molecule. Interestingly, the appearance of lamellar antiferroelectric (SmCP and dark-conglomerate mesophases) and columnar (Col_r) packing, as well as the transition temperatures, can be modulated by using α- or β-moieties.

As one would expect, the multiresponse nature of the cyanostilbene structure means that very appealing photoactivity has been observed in these bent-shaped molecules.

Regarding the SHG efficiencies, bent-core molecules containing cyanostilbene cores on the lateral structures can lead to large first hyperpolarizability values. Thus, an appropriate D–π–A molecular design could allow this kind of molecule to be considered in strategies to afford second order NLO-materials.

The compounds reported here are amongst the rare examples of luminescent bent-core liquid crystals. The β-series compounds show the most marked fluorescence in solution (Φ_{PL} around 8%). Consequently, this sort of compound is not only an innovative fluorescent material with unexplored molecular packing but they also provide fluorescent probes for bent-core mesophase characterization.

In conclusion, the results obtained in this study are very promising in the field of functional materials, either for multiresponsive soft materials or as a tool in the processing and synthesis of functional materials in the solid phase with potential for uses in technological devices and applications. Furthermore, in relation to the properties described here, the presence of the cyanostilbene structure [–Ar–CH═C(CN)–Ar–] enhances these bent-core mesophases by providing photoactivity. In addition, the possibility of photochemical activity provides an alternative to azo (–N═N–) or stilbene (–CH═CH–) materials.

Acknowledgements

This work was financially supported by MICINN-FEDER and MINECO-FEDER of Spain-UE (Projects MAT2011-27978-C02-02 and MAT2012-38538-C03-01 and MAT2012-38538-C03-02) and the Aragón Government and FSE (Project E04), and the JAEPredoc-CSIC program (fellowship to M. Martínez-Abadia) and the Gobierno Vasco (GI/IT-449-10). Thanks are due to Nuclear Magnetic Resonance, Mass Spectra and Thermal Analysis Services from the Instituto de Ciencia de Materiales de Aragón, Universidad de Zaragoza–CSIC (Spain).

Notes and references

1 T. Niori, T. Sekine, J. Watanabe, T. Furukawa and H. Takezoe, *J. Mater. Chem.*, 1996, **6**, 1231–1233.
2 G. Pelzl, S. Diele and W. Weissflog, *Adv. Mater.*, 1999, **11**, 707–724.
3 D. M. Walba, in *Materials-Chirality*, Top. Stereochem., ed. M. M. Green, R. J. M. Nolte, E. W. Meijer, S. E. Denmark and J. Siegel, Wiley, New York, 2003, ch. 8, vol. 24, pp. 457–518.
4 M. Hird, *Liq. Cryst. Today*, 2005, **14**, 9–21.
5 W. Weissflog, H. N. S. Murthy, S. Diele and G. Pelzl, *Philos. Trans. R. Soc., A*, 2006, **364**, 2657–2679.
6 H. Takezoe and Y. Takanishi, *Jpn. J. Appl. Phys., Part 1*, 2006, **45**, 264–625.
7 R. A. Reddy and C. Tschierske, *J. Mater. Chem.*, 2006, **16**, 907–961.
8 G. Pelzl and W. Weissflog, in *Thermotropic Liquid Crystals*, ed. A. Ramamoorthy, Springer, Berlin, 2007, pp. 1–58.
9 A. Jákli, C. Bailey and J. Harden, in *Thermotropic Liquid Crystals*, ed. A. Ramamoorthy, Springer, Berlin, 2007, pp. 59–83.
10 A. Eremin and A. Jákli, *Soft Matter*, 2013, **9**, 615–637.
11 A. Jákli, *Liq. Cryst. Rev.*, 2013, **1**, 65–82.
12 C. Tschierske, *Angew. Chem., Int. Ed.*, 2013, **52**, 8828–8878.
13 *Handbook of Liquid Crystals*, ed. J. W. Goodby, P. J. Collings, T. Kato, C. Tschierske, H. Gleeson and P. Raynes, Wiley-VCH, Weinheim, 2014, vol. 4, part IV.
14 D. R. Link, G. Natale, R. Shao, J. E. Maclennan, N. A. Clark, E. Korblova and D. M. Walba, *Science*, 1997, **278**, 1924–1927.
15 M. B. Ros, J. L. Serrano, M. R. de la Fuente and C. L. Folcia, *J. Mater. Chem.*, 2005, **15**, 5093–5098.
16 J. Etxebarria and M. B. Ros, *J. Mater. Chem.*, 2008, **18**, 2919–2926.
17 C. Zang, N. Diorio and A. Jákli, in *Handbook of Liquid Crystals*, ed. J. W. Goodby, P. J. Collings, T. Kato, C. Tschierske, H. Gleeson and P. Raynes, Wiley-VCH, Weinheim, 2014, vol. 4, pp. 715–742.
18 A. Jákli, I. C. Pintre, J. L. Serrano, M. B. Ros and M. R. de la Fuente, *Adv. Mater.*, 2009, **21**, 3784–3788.
19 A. C. Charif, N. Diorio, K. Fodor-Csorba, J. E. Puskas and A. Jákli, *RSC Adv.*, 2013, **3**, 17446–17452.
20 R. Macdonald, F. Kentischer, P. Warnick and G. Heppke, *Phys. Rev. Lett.*, 1998, **81**, 4408–4411.
21 F. Kentischer, R. Macdonald, P. Warnick and G. Heppke, *Liq. Cryst.*, 1998, **25**, 341–347.
22 C. L. Folcia, I. Alonso, J. Ortega, J. Etxebarria, I. Pintre and M. B. Ros, *Chem. Mater.*, 2006, **18**, 4617–4626.
23 I. C. Pintre, N. Gimeno, J. L. Serrano, M. B. Ros, I. Alonso, C. L. Folcia, J. Ortega and J. Etxebarria, *J. Mater. Chem.*, 2007, **17**, 2219–2227.
24 I. C. Pintre, J. L. Serrano, M. B. Ros, J. Martínez-Perdiguero, I. Alonso, J. Ortega, C. L. Folcia, J. Etxebarria, R. Alicante and B. Villacampa, *J. Mater. Chem.*, 2010, **20**, 2965–2971.
25 B. Champagne, J. Guthmuller, F. Perreault and A. Soldera, *J. Phys. Chem. C*, 2012, **116**, 7552–7560.
26 N. G. Nagaveni, A. Roy and V. Prasad, *J. Mater. Chem.*, 2012, **22**, 8948–8959.
27 C. Keith, R. A. Reddy, M. Prehm, U. Baumeister, H. Kresse, J. L. Chao, H. Hahn, H. Lang and C. Tschierske, *Chem. – Eur. J.*, 2007, **13**, 2556–2577.
28 J. Martínez-Perdiguero, J. Etxebarria, C. L. Folcia, J. Ortega, N. Gimeno and M. B. Ros, *Phys. Rev. E: Stat., Nonlinear, Soft Matter Phys.*, 2010, **82**, 041706.
29 C. L. Folcia, J. Ortega, J. Etxebarria, L. Pan, S. Wang, C. C. Huang, V. Ponsinet, P. Barois, R. Pindak and

N. Gimeno, *Phys. Rev. E: Stat., Nonlinear, Soft Matter Phys.*, 2011, **84**, 010701.
30 N. Vaupotič, D. Pociecha and E. Gorecka, *Top. Curr. Chem.*, 2012, **318**, 281–302.
31 C. Tschierske and D. J. Photinos, *J. Mater. Chem.*, 2010, **20**, 4263–4294.
32 L. E. Hough, M. Spannuth, M. Nakata, D. A. Coleman, C. D. Jones, G. Dantlgraber, C. Tschierske, J. Watanabe, E. Körblova, D. M. Walba, J. E. Maclennan, M. A. Glaser and N. A. Clark, *Science*, 2009, **325**, 452–456.
33 D. M. Walba, L. Eshdat, E. Körblova and R. K. Shoemaker, *Cryst. Growth Des.*, 2005, **5**, 2091–2099.
34 L. E. Hough, H. T. Jung, D. Krueerke, M. S. Heberling, M. Nakata, C. D. Jones, D. Chen, D. R. Link, J. Zasadzinski, G. Heppke, J. P. Rabe, W. Stocker, E. Koerblova, D. M. Walba, M. A. Glaser and N. A. Clark, *Science*, 2009, **325**, 456–460.
35 Y. Hong, J. W. Y. Lam and B. Z. Tang, *Chem. Soc. Rev.*, 2011, **40**, 5361–5388.
36 S. Yamane, K. Tanabe, Y. Sagara and T. Kato, *Top. Curr. Chem.*, 2012, **318**, 395–406.
37 S. S. Babu, V. K. Praveen and A. Ajayaghosh, *Chem. Rev.*, 2014, **114**, 1973–2129.
38 B.-K. An, J. Gierschner and S. Y. Park, *Acc. Chem. Res.*, 2012, **45**, 544–554.
39 L. Zhu and Y. Zhao, *J. Mater. Chem. C*, 2013, **1**, 1059–1065.
40 B. K. An, S. K. Kwon, S. D. Jung and S. Y. Park, *J. Am. Chem. Soc.*, 2002, **124**, 14410–14415.
41 J. Gierschner and S. Y. Park, *J. Mater. Chem. C*, 2013, **1**, 5818–5832.
42 C.-K. Lim, S. Kim, I. C. Kwon, C.-H. Ahn and S. Y. Park, *Chem. Mater.*, 2009, **21**, 5819–5825.
43 X. Zhang, X. Zhang, B. Yang, Y. Yang and Y. Wei, *Polym. Chem.*, 2014, **5**, 5885–5889.
44 J. Kunzelman, M. Kinami, B. R. Crenshaw, J. D. Protasiewicz and C. Weder, *Adv. Mater.*, 2008, **20**, 119–122.
45 J. W. Chung, Y. You, H. S. Huh, B.-K. An, S.-J. Yoon, S. H. Kim, S. W. Lee and S. Y. Park, *J. Am. Chem. Soc.*, 2009, **131**, 8163–8172.
46 S.-J. Yoon, J. W. Chung, J. Gierschner, K. S. Kim, M.-G. Choi, D. Kim and S. Y. Park, *J. Am. Chem. Soc.*, 2010, **132**, 13675–13683.
47 J. W. Chung, S.-J. Yoon, B.-K. An and S. Y. Park, *J. Phys. Chem. C*, 2013, **117**, 11285–11291.
48 M. S. Kwon, J. Gierschner, J. Seo and S. Y. Park, *J. Mater. Chem. C*, 2014, **2**, 2552–2557.
49 J. W. Park, S. Nagano, S.-J. Yoon, T. Dohi, J. Seo, T. Seki and S. Y. Park, *Adv. Mater.*, 2014, **26**, 1354–1359.
50 J. Seo, J. W. Chung, J. E. Kwon and S. Y. Park, *Chem. Sci.*, 2014, **5**, 4845–4850.
51 J. A. Mikroyannidis, A. N. Kabanakis, S. S. Sharma and G. D. Sharma, *Adv. Funct. Mater.*, 2011, **21**, 746–755.
52 S. W. Yun, J. H. Kim, S. Shin, H. Yang, B.-K. An, L. Yang and S. Y. Park, *Adv. Mater.*, 2012, **24**, 911–915.
53 X. Li, Y. Xu, F. Li and Y. Ma, *Org. Electron.*, 2012, **13**, 762–766.
54 S. K. Park, S. Varghese, J. H. Kim, S.-J. Yoon, O. K. Kwon, B.-K. An, J. Gierschner and S. Y. Park, *J. Am. Chem. Soc.*, 2013, **135**, 4757–4764.
55 W. Jia, P. Yang, J. Li, Z. Yin, L. Kong, H. Lu, Z. Ge, Y. Wu, X. Hao and J. Yang, *Polym. Chem.*, 2014, **5**, 2282–2292.
56 V. Percec, A. De Souza Gomes and M. Lee, *J. Polym. Sci., Part A: Polym. Chem.*, 1991, **29**, 1615–1622.
57 J. Tsibouklis, P. H. Richardson, A. M. Ahmed, R. W. Richards, W. J. Feast, S. J. Martin, D. D. C. Bradley and M. Warner, *Synth. Met.*, 1993, **61**, 159–162.
58 H. Aoki, T. Mihara and N. Koide, *Mol. Cryst. Liq. Cryst.*, 2004, **408**, 53–70.
59 R. Bao, M. Pan, J. J. Qiu and C. M. Liu, *Chin. Chem. Lett.*, 2010, **21**, 682–685.
60 R. Bao, M. Pan, Y. Zhou, J. J. Qiu, H. Q. Tang and C. M. Liu, *Synth. Commun.*, 2012, **42**, 1661–1668.
61 S.-J. Yoon, J. H. Kim, K. S. Kim, J. W. Chung, B. Heinrich, F. Mathevet, P. Kim, B. Donnio, A.-J. Attias, D. Kim and S. Y. Park, *Adv. Funct. Mater.*, 2012, **22**, 61–69.
62 W. Mao, K. Chen, M. Ouyang, J. Sun, Y. Zhou, Q. Song and C. Zhang, *Acta Chim. Sin.*, 2013, **71**, 613–618.
63 S. M. Morris, M. M. Qasim, D. J. Gardiner, P. J. W. Hands, F. Castles, G. Tu, W. T. S. Huck, R. H. Friend and H. J. Coles, *Opt. Mater.*, 2013, **35**, 837–842.
64 H. Lu, S. Zhang, A. Ding, M. Yuan, G. Zhang, W. Xu, G. Zhang, X. Wang, L. Qiu and J. Yang, *New J. Chem.*, 2014, **38**, 3429–3433.
65 R. Wei, Y. He, X. Wang and P. Keller, *Macromol. Rapid Commun.*, 2014, **35**, 1571–1577.
66 R. Deb, R. K. Nath, M. K. Paul, N. V. S. Rao, F. Tuluri, Y. Shen, R. Shao, D. Chen, C. Zhu, I. I. Smalyukh and N. A. Clark, *J. Mater. Chem.*, 2010, **20**, 7332–7336.
67 R. Deb, A. R. Laskar, D. D. Sarkar, G. Mohiuddin, N. Chakraborty, S. Ghosh, D. S. S. Rao and N. V. S. Rao, *CrystEngComm*, 2013, **15**, 10510–10521.
68 R. K. Nath, R. Deb, N. Chakraborty, G. Mohiuddin, D. S. Shankar Rao and N. V. S. Rao, *J. Mater. Chem. C*, 2013, **1**, 663–670.
69 R. Deb, M. Oneill, N. V. S. Rao, N. A. Clark and I. I. Smalyukh, *ChemPhysChem*, 2014, **16**, 243–255.
70 M. K. Paul, P. Paul, S. K. Saha and S. Choudhury, *J. Mol. Liq.*, 2014, **197**, 226–235.
71 D. Shen, A. Pegenau, S. Diele, I. Wirth and C. Tschierske, *J. Am. Chem. Soc.*, 2000, **122**, 1593–1601.
72 N. Gimeno, M. B. Ros, J. L. Serrano and M. R. de la Fuente, *Angew. Chem., Int. Ed.*, 2004, **43**, 5235–5238.
73 F. Blockhuys, R. Hoefnagels, C. Peten, C. Van Alsenoy and H. J. Geise, *J. Mol. Struct.*, 1999, **485–486**, 87–96.
74 C. M. L. Vande Velde, F. Blockhuys, C. Van Alsenoy, A. T. H. Lenstra and H. J. Geise, *J. Chem. Soc., Perkin Trans. 2*, 2002, 1345–1351.
75 FFTEM studies carried out by Prof. Clark's group at the University of Colorado, to be published.
76 S. Díez, M. R. de la Fuente, M. A. Pérez-Jubindo and B. Ros, *Liq. Cryst.*, 2003, **30**, 1407–1412.

77 E. Gorecka, N. Vaupotič, D. Pociecha, M. Čepič and J. Mieczkowski, *ChemPhysChem*, 2005, **6**, 1087–1093.
78 J. Ortega, M. R. De la Fuente, J. Etxebarria, C. L. Folcia, S. Díez, J. A. Gallastegui, N. Gimeno, M. B. Ros and M. A. Pérez-Jubindo, *Phys. Rev. E: Stat., Nonlinear, Soft Matter Phys.*, 2004, **69**, 117031.
79 N. Gimeno, J. Barberá, J. L. Serrano, M. B. Ros, M. R. de la Fuente, I. Alonso and C. L. Folcia, *Chem. Mater.*, 2009, **21**, 4620–4630.
80 D. Oelkrug, A. Tompert, H. J. Egelhaaf, M. Hanack, E. Steinhuber, M. Hohloch, H. Meier and U. Stalmach, *Synth. Met.*, 1996, **83**, 231–237.
81 D. Oelkrug, A. Tompert, J. Gierschner, H. J. Egelhaaf, M. Hanack, M. Hohloch and E. Steinhuber, *J. Phys. Chem. B*, 1998, **102**, 1902–1907.
82 J. V. Morris, M. A. Mahaney and J. R. Huber, *J. Phys. Chem.*, 1976, **80**, 969–974.